Computational Fluid Dynamic study of gas mixtures in a Non-Thermal Plasma reactor for CO_2 conversion

Cristina Mas-Peiro [a]* , Fèlix Llovell Ferret [b], Oriol Pou Ibar [a]

[a] Department of Chemical Engineering and Materials Science, IQS School of Engineering, Universitat Ramon Llull, Via Augusta 390, 08017, Barcelona, Spain.

[b] Department of Chemical Engineering, ETSEQ, Universitat Rovira i Virgili, Avinguda Països Catalans 26, 43007, Tarragona, Spain.

Estudio computacional de dinámica de fluidos de mezclas de gases en un reactor de plasma no térmico para la conversión de CO_2.

Estudi de la dinàmica de fluids computacional de mescles de gasos en un reactor de plasma no tèrmic per a la conversió de CO_2.

RECEIVED: 10 JULY 2023; ACCEPTED: 21 DECEMBER 2023; HTTPS://DOI.ORG/10.55815/424061

ABSTRACT

CO_2 utilization has been an emerging technology of increasing global interest due to its direct impact in limiting greenhouse gas emissions. In this contribution, the fluid dynamic behavior of a CO_2 conversion non-thermal plasma (NTP) in a dielectric barrier discharge (DBD) reactor is studied through computational fluid dynamics (CFD) simulations.

Calculations are provided in conjunction with experimental results and the thermodynamic characterization of the compounds and mixtures involved. This CFD study utilizes a well-established methodology that allows the optimization of fluid flow with limited computational burden.

Firstly, results are presented for an Example Case, in which several variables are studied both at the final iteration as well as across iterations. Secondly, a range of Study Cases, changing the inlet composition and volume rate, are presented. Average velocity is one of the most significant variables to predict the reactor's yield, while the temperature, density and pressure in the reactor remain, in most cases, almost constant.

The resulting CFD computations describe the behavior of the fluids in the reactor in a predictive manner for future experimental results. Limitations in the fluid's characterization occur due to not explicitly including the plasma reaction, which will be aimed at in future contributions.

Keywords: CO_2 Conversion, Computational Fluid Dynamics, Dielectric Barrier Discharge Plasma, Fluid Mechanics, Non-Thermal Plasma, Plasma Reactor.

RESUMEN

La utilización de CO_2 ha sido una tecnología emergente de creciente interés mundial debido a su impacto directo en la limitación de las emisiones de gases de efecto invernadero. En esta contribución, se estudia el comportamiento fluidodinámico de un plasma no térmico (NTP) de conversión de CO_2 en un reactor de descarga de barrera dieléctrica (DBD) mediante simulaciones de dinámica de fluidos computacional (CFD).

Los cálculos se proporcionan junto con los resultados experimentales y la caracterización termodinámica de los compuestos y mezclas involucrados. Este estudio CFD utiliza una metodología bien establecida que permite la optimización del flujo de fluidos con una carga computacional limitada.

En primer lugar, se presentan los resultados de un caso de ejemplo, en el que se estudian varias variables tanto en la iteración final como entre iteraciones. En segundo lugar, se presenta una variedad de casos de estudio que cambian la composición de la entrada y el volumen. La velocidad promedio es una de las variables más significativas para predecir el rendimiento

*Corresponding author: cristinamasp@iqs.url.edu

del reactor, mientras que la temperatura, densidad y presión en el reactor permanecen, en la mayoría de los casos, casi constantes.

Los cálculos CFD resultantes describen el comportamiento de los fluidos en el reactor de manera predictiva para futuros resultados experimentales. Las limitaciones en la caracterización del fluido se producen por no incluir explícitamente la reacción del plasma, lo que se abordará en futuras contribuciones**.**

Palabras clave*:* Conversión de CO_2, Dinámica de fluidos computacional, Plasma de descarga de barrera dieléctrica, Mecánica de fluidos, Plasma no térmico, Reactor de plasma.

RESUM

La utilització de CO_2 ha estat una tecnologia emergent d'interès global creixent a causa del seu impacte directe en la limitació de les emissions de gasos d'efecte hivernacle. En aquesta contribució, s'estudia el comportament dinàmic de fluids d'un plasma no tèrmic de conversió de CO_2 (NTP) en un reactor de descàrrega de barrera dielèctrica (DBD) mitjançant simulacions de dinàmica de fluids computacional (CFD).

Els càlculs es proporcionen conjuntament amb els resultats experimentals i la caracterització termodinàmica dels compostos i mescles implicats. Aquest estudi CFD utilitza una metodologia ben establerta que permet l'optimització del flux de fluids amb una càrrega computacional limitada.

En primer lloc, es presenten els resultats d'un cas exemple, en el qual s'estudien diverses variables tant a la iteració final com a través de les iteracions. En segon lloc, es presenten una sèrie de casos d'estudi, canviant la composició d'entrada i la velocitat de volum. La velocitat mitjana és una de les variables més significatives per predir el rendiment del reactor, mentre que la temperatura, la densitat i la pressió al reactor es mantenen, en la majoria dels casos, gairebé constants.

Els càlculs CFD resultants descriuen el comportament dels fluids al reactor de manera predictiva per a futurs resultats experimentals. Les limitacions en la caracterització del fluid es produeixen perquè no s'inclou explícitament la reacció del plasma, a la qual s'orientarà en futures contribucions.

Paraules clau*:* Conversió de CO_2, Dinàmica de fluids computacional, Plasma de descàrrega de barrera dielèctrica, Mecànica de fluids, Plasma no tèrmic, Reactor de plasma

INTRODUCTION

The current increase in energy demand has led to the intensive use of fossil fuels, increasing the amount of anthropogenic carbon dioxide (CO_2) emissions to the atmosphere. As one of the most significant greenhouse gases, CO_2 is one of the biggest contributors to global warming [1]. The development of CO_2 capture, storage, usage, and conversion (CCUS) technologies has therefore become of growing interest. CCUS processes play an important role in net-zero energy systems, as they contribute to both reducing and utilizing CO_2 emissions [2].

CO_2-utilization technologies can be understood as either a direct utilization or a conversion to other chemicals and energy products. In the case of direct utilization, CO_2 is used, for instance, as a: commercial product in the food and beverage industry, supercritical CO_2 as a solvent, among other industrial applications [3].

With CO_2 conversion, CO_2 can be converted into other chemicals or energy products through carboxylation reactions in which a CO_2 molecule is used to obtain organic compounds, (including carbonates, acrylates, and polymers) or through reduction reactions where the C=O bonds are broken to produce other chemicals (including methane, methanol, urea, syngas, and formic acid) [4], [5].

In fact, CO_2 conversion has evolved to cover a wide range of technologies, including hydrogenation [6], electro-catalytic / electrochemical reduction [4], enzymatic / biochemical [4], photo-reduction [4], [7], [8] or plasma processes [1], [9]–[11]. One plasma process of particular interest is non-thermal plasma (NTP), due to its capability to break down the OC=O bond via stepwise vibrational excitation. NTP plasmas can be operated at room temperature and atmospheric pressure, a major advantage in comparison to traditional techniques which require high temperature (1600-2000K) and/or pressure working conditions [12].

This study focuses on the specific application of a NTP for CO_2 decomposition into carbon monoxide (CO) and oxygen (O_2), with the usage of argon (Ar) as diluent gas. The plasma reactor from experimental results is a dielectric barrier discharge (DBD) reactor packed with copper-based pellets as catalysts [13].

The plasma is generated by applying a potential difference between two electrodes, which are inserted in a reactor filled with gas [12], [14]. When electrons are accelerated by the electric field generated, they collide towards gas molecules, resulting in ionization, excitation, and dissociation. The dissociation collisions create radicals, which can form new compounds. It is under this principle that gas conversion applications occur.

The dissociation of the CO_2 molecule is not spontaneous, as it is thermodynamically a highly stable molecule, with a Gibbs free energy of 397kJ/mol. A significant energy input is required to break the OC=O double bond and dissociate the molecule. In NTP dissociation, the energy required can be achieved solely through electric power at atmospheric conditions. The electrons produced in the plasma acquire high energies, between 1 and 10 eV [13].

Research shows that the use of Ar as a diluent gas proves beneficial in CO_2 conversion. As the minimum voltage required to form plasma with Ar is lower than for CO_2 reactant, the excited Ar atoms can provide charge/energy transfer to CO_2 molecules [15].

Previous literature has shown the potential of Computational Fluid Dynamics (CFD) simulations in rep-

resenting fluid mechanics behavior in a diverse range of reactors, including CO_2 conversion reactors such as the one in our study.

A good overview of CFD approaches, from mathematical models to software strategies, for the analysis of atmospheric pressure plasmas is presented in previous works [16], where the fidelity (if relevant phenomena are not accounted for) and accuracy (if numerical approximation is inappropriate) challenges of CFD are tackled to increase the predictive capability of numerical simulations towards comparable to experimental results.

Research Group PLASMANT has provided several contributions of plasma-based CO_2, CH_4 or N_2 conversion studies [17], [18], most notably the CFD analysis of a dual-vortex plasmatron, a gliding arc (GA) plasma reactor with specific electrode configuration [19]. The fluid dynamic simulations show a strong rotational gas flow in the novel reactor concept, as one of the elements impacting the CO_2 conversion rate. Previous contributions [20] from the same research group have shown the transverse 2D modelling of a GA reactor, providing a deep understanding of the gas-discharge interaction through computational fluid dynamics.

Other research groups have also been able to implement CFD simulations for a thermal rotating arc reactor, showing satisfactory simulations representing the reactor's behavior and possible parameters affecting its performance [21]. This is also the case for studies of plasmas [22] with a design of convergent-divergent nozzles discharging high-temperature plasma jets, in which a computational fluid dynamic analysis of 55 models with different cross-sectional profiles for the optimization of plasma configuration is completed.

Literature of non-thermal plasma reactors with a dielectric barrier discharge (DBD) is also found for NOx reduction applications in a cylindrical reactor with high voltage-ground electrodes [23]. This work of fluid mechanics provides an understanding of the electric field distribution in the reactor and the impacts of several parameters, including reactor design, dielectric properties, and thickness.

Other plasma studies have also shown satisfactory results with computational fluid dynamics modelling, such as a cold plasma methane reformer reactor in which a 3D gliding arc vortex reformer is investigated [24]. The effects of geometry and confirmation on the reformer performance for partial oxidation of methane to produce syngas are simulated. Similar results have been found for a methane dry reforming reactor over a Ni/Al_2O_3 catalyst with a spark plasma [25], in which computational dynamics modelling is successfully linked to reaction kinetic modelling.

In the present study, a CFD model for a CO_2 conversion non-thermal plasma (NTP) dielectric barrier discharge (DBD) reactor is developed to optimize fluid flow for CO conversion rate. The goal is to strengthen the correlation between the CFD behavior and the current experimental results, taking advantage of the limited computational burden of the simulations to enhance future experimental tests.

For this aim, firstly, the experimental results from Research Group GESPA are considered [13], in which the conversion of CO_2 to CO via a catalyst-packed reactor has been studied. The computational study utilizes the basis of this laboratory work to specify the reactor set-up, dimensions and working conditions. The compounds involved are CO_2, CO, O_2, and Ar (as well as additional impurities). It is significant to note that the computational simulations in this work are simplified with only the reactants as inputs (thus, CO_2 and Ar). The experimental results provide a yield (%) depicting maximum CO conversion, considering several input variables (CO_2 inflow rate, applied voltage and frequency, copper catalyst concentration, gap between electrodes, as well as inlet composition).

Secondly, the thermodynamic characterization of gas mixtures involved shown in previous contributions is extrapolated to experimental working conditions and introduced in the model [26]. This thermodynamic behavior has been studied with a polar soft-SAFT EoS and depicts primary compounds, binary mixtures and ternary mixtures of the elements and impurities involved (CO_2, O_2, CO, Ar, N_2, H_2) [27].

This contribution results from the preliminary results [28] presented depicting the CFD behavior in a simplified 3D geometry of the reactor for a specific inlet flow rate and composition. The model in this contribution aims to understand the effects of reactor design and gas inlet (flow rate, composition) in optimizing fluid flow. It is significant to note, that the CFD model has great adaptability to compute several cases with few computational limitations, however, the simplicity of the model does not consider the plasma reactions (and involved phenomena) explicitly.

METHODOLOGY

To characterize the gas flow behavior in the reactor, this study develops a CAD 3D Geometry with SolidWorks® and introduces a gas flow model with the SolidWorks® Flow Simulation module. The flow simulation approach implements the direct use of native CAD as the source of geometry information, which is then combined with full 3D CFD modelling. The SolidWorks® Flow Simulation module incorporates: CAD data management, Mesh generation, CFD solvers, Engineering Modelling Technologies, and Results Processing [29].

1. Governing Equations

Just like other CFD software, SolidWorks® Flow Simulation [29] solves the Navier-Stokes equations as formulations of mass and momentum conservation laws. These describe how the velocity, pressure, and density of a moving fluid are related.

In fluid regions, the governing equations are as follows:

$$\nabla \cdot \mathbf{P} + f = \rho \frac{\partial \boldsymbol{u}}{\partial t} + \rho(\boldsymbol{u} \cdot \nabla)\boldsymbol{u} \quad (1)$$

$$\frac{\partial \rho}{\partial t} + \nabla \cdot (\rho \boldsymbol{u}) = 0 \quad (2)$$

Table 1. *Inlet Boundary Conditions (BC) ranges for CFD Study Cases*

	Inlet Volume Flow Rate [L/min]			Inlet Volumetric Composition (%)	
Boundary Condition	Ar	CO_2	Total	Ar	CO_2
Range	0.5 - 1	0.003 – 0.045	0.503 – 1.045	95.69 – 99.70	0.03 – 4.31

where **P** stands for the Cauchy stress tensor, f the fluid body force, ρ the fluid density and $\boldsymbol{u}$ the gas flow vector.

The tool considers both laminar and turbulent flows. If turbulent flow occurs, the description employs transport equations for the turbulent kinetic energy and its dissipation rate, following the so-called k-ε model.

The SolidWorks® Flow Simulation module uses Cartesian-based meshes, which, as a result have cells that are located fully in solid bodies (solid cells), in the fluid (fluid cells) and cells intersected in the immersed boundary ('partial cells'), which allows a calculation using a single mesh computation.

2. Computational Domain and Mesh

The computational domain is based on the reactor geometry from the experimental set-up in a 3D Geometry [13]. It includes the entire fluid region and the solid components that interface with fluid.

The main reactor components are: **1)** Inner Rod (anode), **2)** Outer Mesh (cathode), **3)** Dielectric Barrier Discharge (Quartz), **4)** Inlet Teflon Part (PTFE), **5)** Outlet Teflon Part (PTFE), and **6)** Catalyst (copper-based CuO/ZnO). The cross-section of this 3D Model including the Computational Domain and Basic Mesh is provided in Figure 1. For reference, basic measurements include: L_{Core} = 210 [mm], R_{Core} = 4.5 [mm], R_{inlet} = 4.5 [mm], and R_{outlet} = 4.5 [mm].

The particles that define the catalyst-packed reactor are represented as a porous medium. In an experimental setting, the copper-based catalysts (pellets, 5.4mm x 3.6mm) are introduced as packaging in the reactor, but the simulation introduces the catalyst as a non-solid porous medium with an orthotropic behavior of 57.4% porosity (as obtained in laboratory tests). The porous medium is introduced in the Engineering Database as a user-defined porosity.

Adequate meshing will determine the accuracy of the results, but a mesh that is too refined can result in significant computational burdens. For the initial results, an automatic mesh function was used (Level of Initial Mesh: 4 at a minimum), which was then manually refined, especially at the inlet and outlet points, or for cases that require further finesse.

3. Simulation Set-Up and Boundary Conditions

The flow simulation set-up includes additional assumptions to describe the fluid flow behavior. Firstly, the two reactant fluids involved (CO_2 and Ar) are introduced as user-defined fluids from previous thermodynamic characterization. These are defined in the Engineering Database (Materials > Gases), specifying: dynamic viscosity [Pa·s], specific heat C_p [J/ kg·K], thermal conductivity [W/(m·K)] vs. Temperature [K]. However, as no thermal reaction is introduced, considering it is a non-thermal plasma, the changes in fluid temperature will result to be almost negligible.

Secondly, a set of goals are specified in the simulation tool, which in this case have only been global goals. The specified global goal targets are min./max./avg. for pressure, velocity, fluid density, dynamic viscosity, fluid temperature, and vorticity.

Thirdly, the following boundary conditions are considered: volume flow rate and substance composition at the inlet, and environmental pressure at the outlet. Once the first case is built with a specific inlet flow rate and composition (**Example Case**: (1) inlet flow rate = 1.015 [L/min], (2) CO_2/Ar mixture = 1.48/98.52%), a range of **Study Cases** of fluid dynamics can be completed changing the inlet variables to optimize fluid flow. The range of the inlet boundary conditions for the **Study Cases** can be found in Table 1. These ranges result in 36 case studies and are aligned with the experimental results to be directly compared.

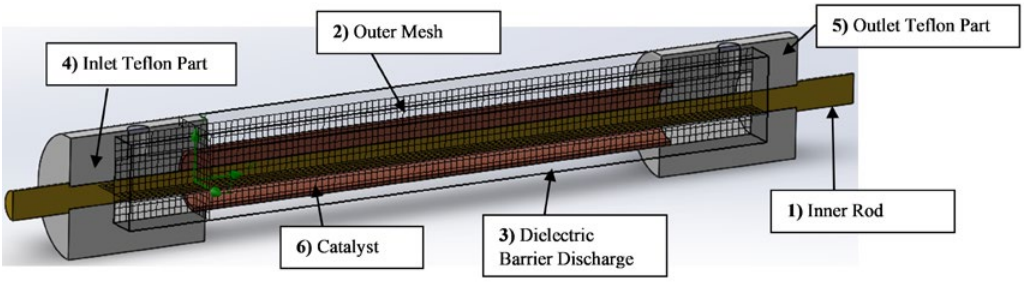

Figure 1. *Cross-section of 3D Model of Reactor with Computational Domain and Mesh*

Additional assumptions have been made in the flow simulation, such as not including a heat induction source, allowing both laminar and turbulent flow in the computation, not including the plasma reaction to concentrate solely on the CFD behavior of the mixture.

RESULTS AND DISCUSSION

The results presented below include firstly a full understanding of the **Example Case**, as specified above, and then a comprehensive overview of the **Study Cases** in the specified ranges.

1. Example Case

The initial computational fluid characterization is provided for a specific **Example Case** (1) inlet flow rate = 1.015 [L/min], (2) CO_2/Ar mixture = 1.48/98.52%). The initial automatic mesh (Level of Initial Mesh (5)) is solved in 185 iterations. When compared to experimental results, **Example Case** provides a 23.41% (+/- 6.64%) yield in the reactor.

1.1 Velocity in Flow Particles

In Figure 2 the behavior of the fluid velocity is represented in flow particles. It is noted that the highest velocity is found at the inlet/outlet ends (maximum at around 0.296 [m/s]). It decreases when the PTFE ends, where no plasma occurs (no cathode/anode interaction), reaching the lowest velocity (minimum at around 0.005 [m/s]). The velocity alongside the copper core remains almost constant at 0.114 [m/s].

It is important to note that the particle flow travels homogeneously across the pellets, allowing adequate fluid mixture between cathode/anode. The even, orthotropic flow obtained due to the user-defined porous medium is a simplification of experimental results with uneven flow.

The velocity is one of the most significant elements to consider towards reactor's performance from a fluid dynamic perspective. Too high a velocity may not allow enough time for efficient plasma reactions, but too slow a velocity might limit the ignition of the plasma (with Ar as the diluent gas).

1.2 Vorticity in Surface Contour

Another variable of importance is the vorticity, representing the rotational motion of the fluid in the reactor. In Figure 3 the vorticity is represented as a surface contour. Vorticity reaches its lowest value alongside the copper core and starts to increase once leaving/entering the PTFE ends. Constant low vorticity along the reactor (47.17 [1/s]) allows adequate fluid mixture for reactor efficiency.

An excessively high rotational motion would facilitate mixing but might impediment efficient plasma reactions, affecting the CO conversion rate. The constant vorticity across the reactor is expected, due to the porous catalyst being introduced as orthotropic medium.

1.3 Temperature in Cut Contour

An additional variable of interest is the temperature of the fluid. As represented in Figure 4, the temperature variation of the fluid mixture is minimal, maintained at room temperature (293.20 [K]). This is representative of the reactor's behavior, even if the plasma calculations have not been explicitly computed, as it operates at atmospheric pressure and room temperature.

Even with minimal variation, the fluid temperature reaches its maximum value in the inlet upon reaching the copper rod. The fluid temperature along the bottom of the rod is slightly higher than the temperature along the top. This uneven behavior is due to the placing of the inlet and outlet ends.

This is particularly interesting when considering the thermodynamic behavior of the CO_2/Ar mixture. Previous contributions have shown that at 293.2 [K] vapor-liquid equilibrium of a CO_2/Ar mixture cannot be reached with the given composition (CO_2/Ar mixture = 1.48/98.52%). However, at lower temperatures

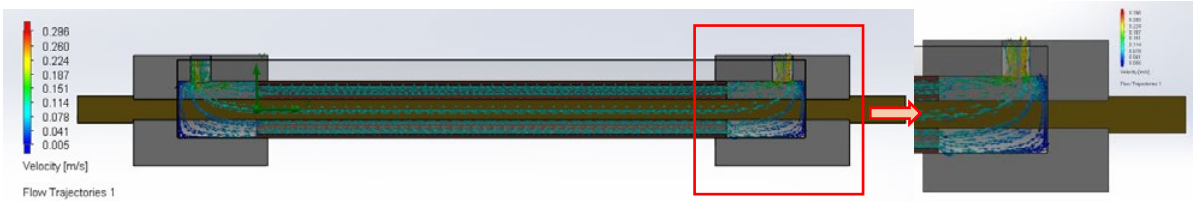

Figure 2. *Fluid Velocity [m/s] in Flow Particles for Example Case*

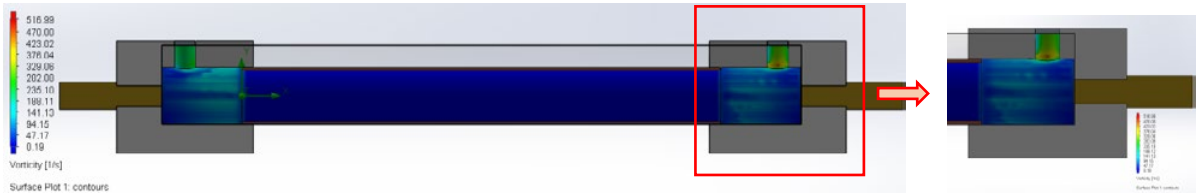

Figure 3. *Vorticity [1/s] in Surface Contour for Example Case*

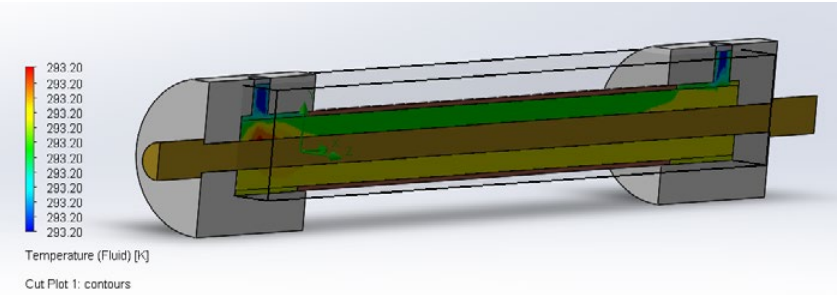

Figure 4. *Fluid Temperature [K] in Cut Plot Contour for Example Case*

(<293.20 [K]), higher pressures (0-16 [MPa]) and with higher proportion of CO_2 (20-100%), VLE could be reached [26], negatively affecting the performance of the plasma.

1.4 Velocity, Dynamic Viscosity, Total Pressure and Density through Iterations

Previous results have considered only the final iteration of the CFD computations. An additional perspective is given with the understanding of the development of these variables throughout iterations. Several global goals have been selected below (average: velocity [m/s], dynamic viscosity [Pa·s], total pressure [Pa], and fluid density [kg/m^3]) in Figure 5.

Firstly, the average velocity through iterations indicates a large drop from the initial entry velocity. It reaches its lowest value almost at 0.0764 [m/s] at around iteration 30, which then recovers to a stable final value. This is the overall velocity throughout the reactor; an analogous behavior would be expected in the inlet and outlet with differing velocity magnitudes.

Secondly, the dynamic viscosity of the fluid is considered. The climb starts at around 40 iterations reaching its highest value at iteration 80. Dynamic viscosity is the measure of fluid resistance to flow when an external force is applied; hence, in this sense, the fluid's resistance increases due to the movement introduced in the reactor, which finally stabilizes.

a) *b)*

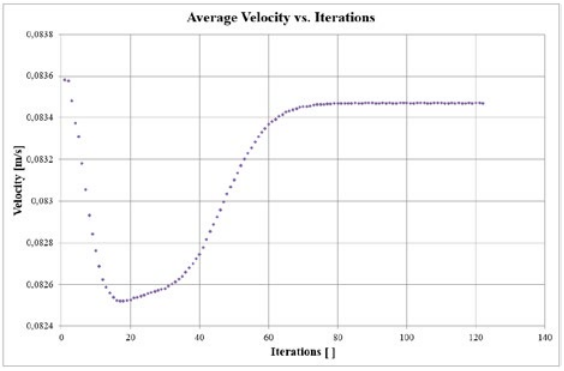

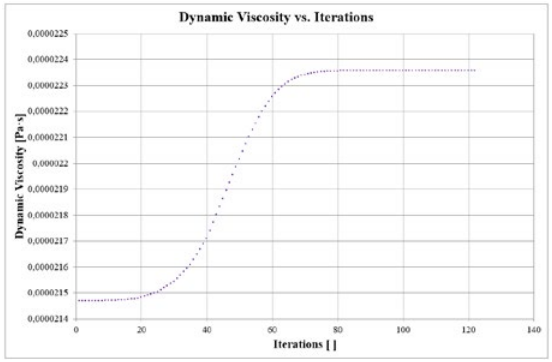

c) *d)*

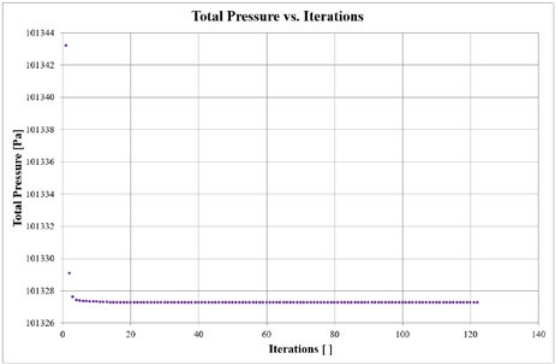

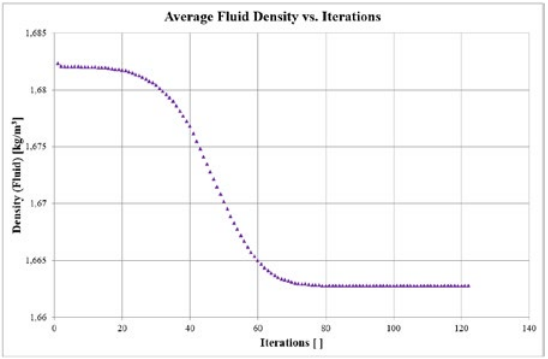

Figure 5. *Global Goals across Computational Iterations* **a)** *Average Velocity [m/s],* **b)** *Average Dynamic Viscosity [Pa·s],* **c)** *Average Total Pressure [Pa], and* **d)** *Average Fluid Density [kg/m^3]*

Thirdly, the steep drop in average pressure across the iterations can be observed. Previous computations for the **Example Case** have shown that the drop across the reactor length is almost negligible (4.84 [Pa]). Pressure stability is indicative of a main advantage of the NTP-reactor, which can be operated at atmospheric pressure.

Finally, the drop in average density is achieved after few iterations, starting with a stark decline at 40 iterations until 80, where it reaches its final average density (1.668 [kg/m^3]) that is stable until the final computations. As with the fluid temperature, the density computation is of particular interest considering the thermodynamic characterization of the CO_2/Ar mixture. For instance, pure Argon at 298.20 [K] and atmospheric pressure (101,325 [Pa]) has a density of 1.6283 [kg/m^3], while pure CO_2 has a density of 1.8018 [kg/m^3], which, considering the mixture's composition, is comparable to the fluid simulation results [31].

2. Computational Study Cases

In this section, different **Study Cases** are presented, as specified in Table 2, differing in gas mixture composition and total inlet volume flow rate resulting in 36 calculations. All CFD cases are compared to experimental results, most significantly the yield (%), to specify the optimization of fluid flow.

2.1 Average and Circumferential Velocity

The first element to consider is the direct linear correlation that is found between the average velocity and the volumetric composition (%) at a constant inlet volume rate. This can be observed in Figure 6 with studies increasing in argon composition.

This correlation allows us to directly link the reactor yield (%) to the average velocity at a constant inlet volume rate across all CFD computations, which can be seen in Figure 7, enabling an understanding of the optimization of fluid flow. For instance, at a constant total inlet volume rate of 1 L/min, a considerable change in

Table 2. *Study Cases Overview*

	Inlet Volume Rate [L/min]			Composition		Reactor Yield (%)
	Ar	CO_2	Total	Ar	CO_2	Yield (%)
1	1	0,045	1,045	0,9569	0,0431	4,55
2	1	0,036	1,036	0,9653	0,0347	6,11
3	1	0,03	1,03	0,9709	0,0291	8,80
4	1	0,021	1,021	0,9794	0,0206	14,31
5	1	0,015	1,015	0,9852	0,0148	23,42
6	1	0,015	1,015	0,9852	0,0148	20,98
7	1	0,009	1,009	0,9911	0,0089	40,24
8	1	0,009	1,009	0,9911	0,0089	49,32
9	1	0,006	1,006	0,9940	0,0060	55,40
10	1	0,006	1,006	0,9940	0,0060	64,45
11	1	0,003	1,003	0,9970	0,0030	74,17
12	1	0,003	1,003	0,9970	0,0030	75,49
13	0,86	0,015	0,865	0,9827	0,0173	13,49
14	0,86	0,009	0,859	0,9895	0,0105	39,00
15	0,86	0,006	0,856	0,9930	0,0070	51,00
16	0,86	0,003	0,853	0,9965	0,0035	59,10
17	0,75	0,015	0,765	0,9804	0,0196	11,70
18	0,75	0,009	0,759	0,9881	0,0119	32,42
19	0,75	0,006	0,756	0,9921	0,0079	34,55
20	0,75	0,003	0,753	0,9960	0,0040	43,85
21	0,7	0,015	0,715	0,9790	0,0210	8,37
22	0,7	0,009	0,709	0,9873	0,0127	27,88
23	0,7	0,006	0,706	0,9915	0,0085	24,04
24	0,7	0,003	0,703	0,9957	0,0043	35,06
25	0,65	0,015	0,665	0,9774	0,0226	6,00
26	0,65	0,009	0,659	0,9863	0,0137	21,72
27	0,65	0,006	0,656	0,9909	0,0091	20,77
28	0,65	0,003	0,653	0,9954	0,0046	30,03
29	0,6	0,015	0,615	0,9756	0,0244	4,81
30	0,6	0,009	0,609	0,9852	0,0148	18,25
31	0,6	0,006	0,606	0,9901	0,0099	18,01
32	0,6	0,003	0,603	0,9950	0,0050	18,91
33	0,5	0,015	0,515	0,9709	0,0291	3,78
34	0,5	0,009	0,509	0,9823	0,0177	13,02
35	0,5	0,006	0,506	0,9881	0,0119	9,82
36	0,5	0,003	0,503	0,9940	0,0060	13,67

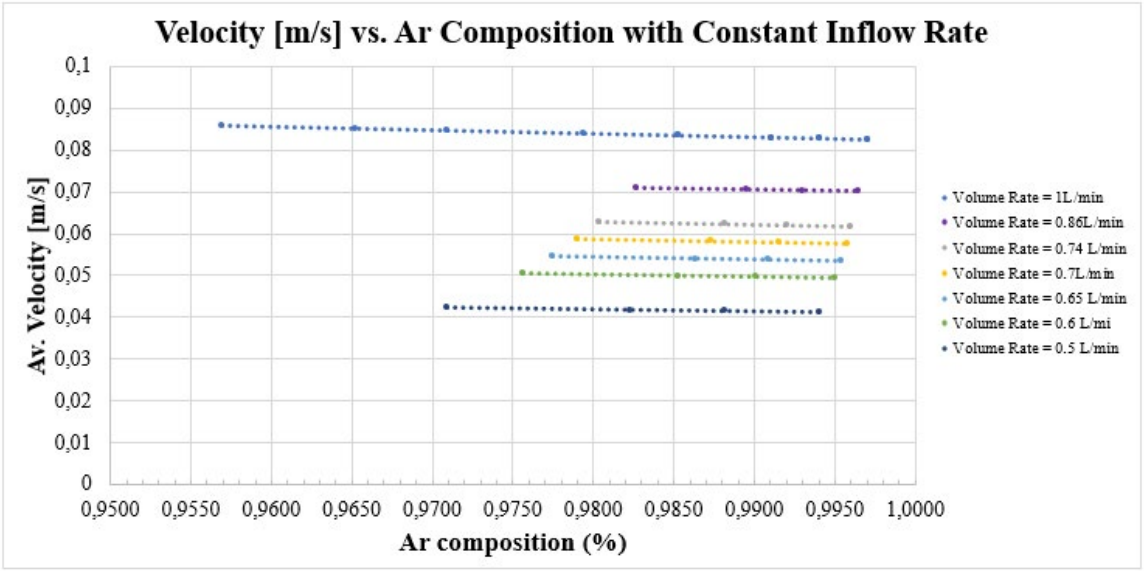

Figure 6. *Av. Velocity [m/s] vs. Ar Composition (%) with Constant Inlet Volume Rate*

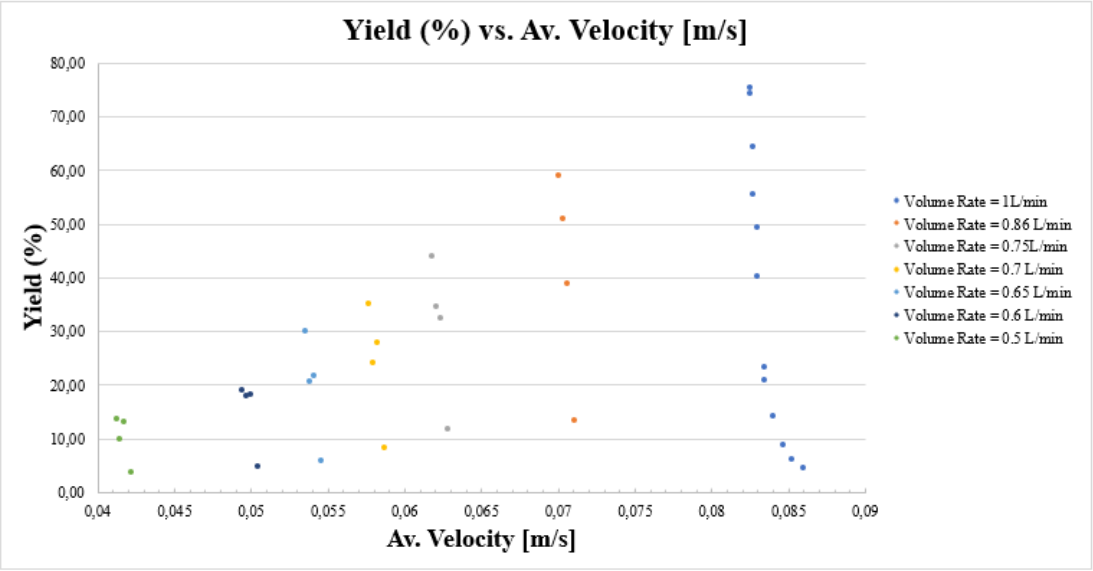

Figure 7. *Yield (%) vs. Av. Velocity [m/s] at Constant Inlet Volume Rate*

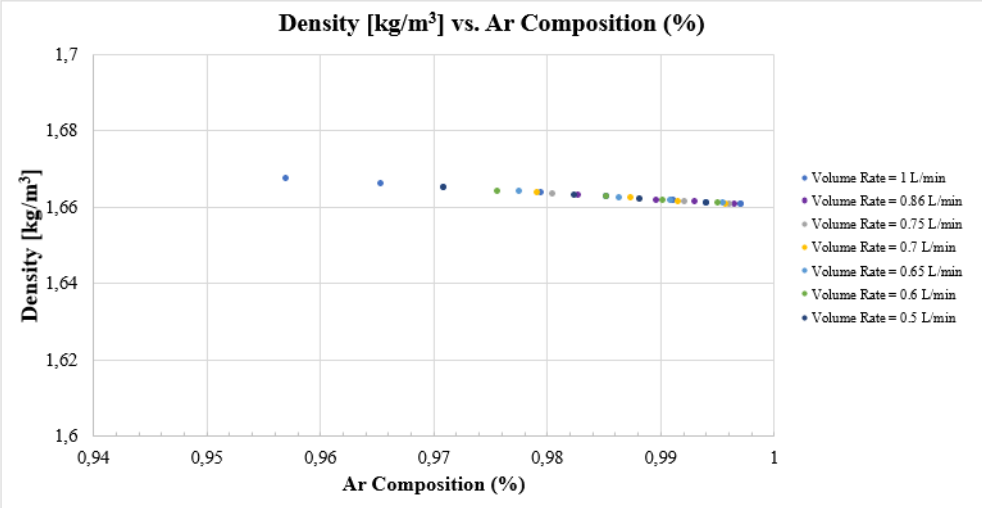

Figure 8. *Density (kg/m³) vs. Ar Composition (%) at Constant Inlet Volume Rate*

reactor conversion can be found with changing average velocity; at the lowest velocity (82.48 [mm/s]) the reactor provides the highest yield (75.49%); in comparison, at the highest velocity (85.95 [mm/s]), the reactor obtains a performance of 4.55%. Computing the average velocity with a specific Ar % and volume inlet rate could allow a direct prediction of the reactor yield.

The difference in reactor conversion performance is considerable and directly related to the volumetric concentration of argon. It is presumable that with a further increase in Ar % an improved yield would be obtained, due to enabling the forming of plasma. However, the CO_2 % cannot be too low, since the conversion to CO then cannot occur. At the same inlet rate and composition, a slightly lower velocity shows a better performance, since the plasma has the time to affect the compounds in the compounds involved (and cause the ionization reactions).

As with the **Example Case**, the velocity is a key indicator of the plasma's conversion rate. A similar behavior is observed with circumferential velocity across the **Study Cases**, although the values differ in magnitude.

2.2 Fluid Density

When observing the fluid density, seen in Figure 8, this remains, as expected, almost constant with increasing argon composition. It is significant to note that it is fully independent of the inlet volume rate. The density value is in between the density of pure Ar and pure CO_2 (at ambient temperature and atmospheric pressure) and decreases as the Ar composition increases (thus approaching the density value at pure Ar).

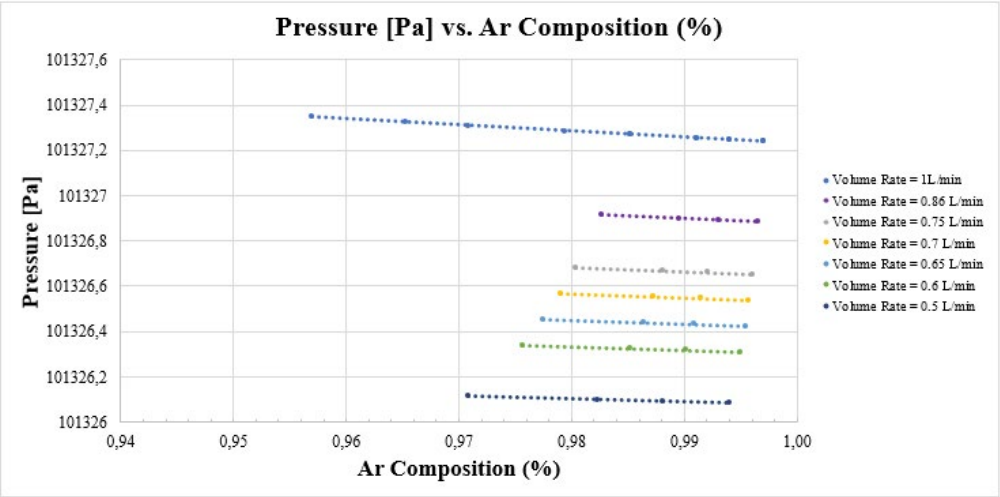

Figure 9. *Pressure (Pa) vs. Ar Composition (%) at Constant Inlet Volume Rate*

2.3 Pressure

Similarly, the behavior of the pressure is presented below in Figure 9.

As previously mentioned, the pressure is almost maintained at a constant value throughout all **Study Cases**. It shows a linear behavior to the Ar composition. This is as expected since the velocity has shown a similar correlation. As with the velocity, the pressure can be an indicator of the performance of the reactor, for future experimental tests.

CONCLUSION

In this work, the fluid dynamic study of a non-thermal CO_2 conversion reactor has been studied through computational fluid dynamic studies. These results have been compared to the available experimental results of the same reactor, to show if a simple CFD approach can allow an optimization of fluid flow.

Firstly, an initial **Example Case** is presented, where a CFD simulation is presented, commenting on: average velocity, vorticity and fluid temperature. Most notably, the velocity is a key element in understanding the reactors performance. Too high a velocity can jeopardize the ionization reactions in the plasma, as the involved compounds travel too quickly across the reactor. This **Example Case** is also studied throughout computational iterations for additional variables (dynamic viscosity, pressure, density, and average velocity). The resolution of computational iterations is achieved without difficulty, but some variables find their points of stability at earlier iterations, in comparison to others. For instance, the pressure drop is almost instantaneous, while the stabilization of the density requires half of the iteration times.

Secondly, through a range of **Study Cases** differing in the inlet volume rate and the composition, additional CFD characterization is provided. The different computations allow a comparison between the variables and yield, as is the case with the average velocity at constant inlet volume rate. The understanding of the velocity across the reactor can allow a comparison with experimental results and the yield of the reactor in a predictive manner. Additional variables studied are the fluid density and pressure which, as expected, remain practically constant across all cases.

These computational simulations provide a strong basis for the optimization of the fluid flow in the reactor. Future work can include the extension of these computations to a direct comparison with experimental results in a laboratory setting

In addition, as stated, the CFD simulations simplify the calculations by not introducing the plasma reaction. Thus, further contributions could be addressed at the plasma physics and occurring reactions, relevant for CO_2 decomposition with Ar as an ionized gas (Ar+). The introduction of plasma physics must be addressed with other commercial products that consider Multiphysics interactions, where the behavior of the plasma is compounded into this CFD characterization.

ACKNOWLEDGEMENTS

The authors acknowledge the financial support to this work from the Spanish Ministry of Science and Innovation MCIN/AEI/10.13039/501100011033/under R + D + I project STOP-F-Gas (Ref: PID2019-108014RB-C21). GESPA (2021 SGR 00321) and AGACAPE (2021 SGR 00738) have been recognized as Consolidated Research Groups by the Catalan Government. Additional funding from 2021 SGR 00738 is also acknowledged.

REFERENCES

1. Q. Zhu, "Developments on CO2-utilization technologies," *Clean Energy*, vol. 3, no. 2, pp. 85–100, May 2019, doi: 10.1093/ce/zkz008.
2. IEA World Energy Outlook 2022, "World Energy Outlook 2022," Paris, 2022. Accessed: Jul. 03, 2023.

[Online]. Available: https://www.iea.org/reports/world-energy-outlook-2022
3. C.-H. H. Huang and C.-S. S. Tan, "A Review: CO2 Utilization," *Aerosol Air Qual Res*, vol. 14, no. 2, pp. 480–499, 2014, doi: 10.4209/aaqr.2013.10.0326.
4. P. R. Yaashikaa, P. Senthil Kumar, S. J. Varjani, and A. Saravanan, "A review on photochemical, biochemical and electrochemical transformation of CO2 into value-added products," *Journal of CO2 Utilization*, vol. 33, pp. 131–147, 2019, doi: 10.1016/j.jcou.2019.05.017.
5. P. Markewitz *et al.*, "Worldwide innovations in the development of carbon capture technologies and the utilization of CO2," *Energy Environ Sci*, vol. 5, no. 6, pp. 7281–7305, 2012, doi: 10.1039/C2EE03403D.
6. S. Saeidi, N. A. S. Amin, and M. R. Rahimpour, "Hydrogenation of CO2 to value-added products—A review and potential future developments," *Journal of CO2 Utilization*, vol. 5, pp. 66–81, 2014, doi: 10.1016/j.jcou.2013.12.005.
7. B. Kumar, M. Llorente, J. Froehlich, T. Dang, A. Sathrum, and C. P. Kubiak, "Photochemical and Photoelectrochemical Reduction of CO2," *Annu Rev Phys Chem*, vol. 63, no. 1, pp. 541–569, Apr. 2012, doi: 10.1146/annurev-physchem-032511-143759.
8. A. A. Khan and M. Tahir, "Recent advancements in engineering approach towards design of photo-reactors for selective photocatalytic CO2 reduction to renewable fuels," *Journal of CO2 Utilization*, vol. 29, pp. 205–239, 2019, doi: 10.1016/j.jcou.2018.12.008.
9. D. Mei and X. Tu, "Conversion of CO2 in a cylindrical dielectric barrier discharge reactor: Effects of plasma processing parameters and reactor design," *Journal of CO2 Utilization*, vol. 19, pp. 68–78, 2017, doi: 10.1016/j.jcou.2017.02.015.
10. M. Ramakers, I. Michielsen, R. Aerts, V. Meynen, and A. Bogaerts, "Effect of Argon or Helium on the CO2 Conversion in a Dielectric Barrier Discharge," *Plasma Processes and Polymers*, vol. 12, no. 8, pp. 755–763, Aug. 2015, doi: 10.1002/ppap.201400213.
11. J. Amouroux, S. Cavadias, and A. Doubla, "Carbon Dioxide reduction by non-equilibrium electrocatalysis plasma reactor," *IOP Conf Ser Mater Sci Eng*, vol. 19, p. 12005, 2011, doi: 10.1088/1757-899x/19/1/012005.
12. R. Snoeckx and A. Bogaerts, "Plasma technology-a novel solution for CO2 conversion?," *Chem Soc Rev*, vol. 46, no. 19, pp. 5805–5863, 2017, doi: 10.1039/c6cs00066e.
13. J. O. Pou, C. Colominas, and R. Gonzalez-Olmos, "CO2 reduction using non-thermal plasma generated with photovoltaic energy in a fluidized reactor," *Journal of CO2 Utilization*, vol. 27, pp. 528–535, 2018, doi: 10.1016/j.jcou.2018.08.019.
14. A. Bogaerts, T. Kozák, K. van Laer, and R. Snoeckx, "Plasma-based conversion of CO2: current status and future challenges," *Faraday Discuss*, vol. 183, no. 0, pp. 217–232, 2015, doi: 10.1039/C5FD00053J.
15. D. Ray, R. Saha, and S. Ch, "DBD Plasma Assisted CO 2 Decomposition : Influence of Diluent Gases," pp. 1–11, 2017, doi: 10.3390/catal7090244.
16. J. P. Trelles, "Advances and challenges in computational fluid dynamics of atmospheric pressure plasmas," 2014.
17. K. Van Laer and A. Bogaerts, "Fluid modelling of a packed bed dielectric barrier discharge plasma reactor," *Plasma Sources Sci Technol*, vol. 25, no. 1, Dec. 2015, doi: 10.1088/0963-0252/25/1/015002.
18. A. Bogaerts, R. Snoeckx, G. Trenchev, and W. Wang, "Modeling for a Better Understanding of Plasma-Based CO 2 Conversion." [Online]. Available: www.intechopen.com
19. G. Trenchev and A. Bogaerts, "Dual-vortex plasmatron: A novel plasma source for CO2conversion," *Journal of CO2 Utilization*, vol. 39, Jul. 2020, doi: 10.1016/j.jcou.2020.03.002.
20. A. F. Gutsol and S. P. Gangoli, "Transverse 2-D gliding arc modeling," *IEEE Transactions on Plasma Science*, vol. 45, no. 4, pp. 555–564, Apr. 2017, doi: 10.1109/TPS.2017.2653841.
21. S. G. Johnsen, S. G. Johnsen, and A. J. Simonsen, "CFD MODELING OF A ROTATING ARC PLASMA REACTOR SFI Metal Production View project Virtual Surgery in the Upper Airways-New Solutions to Obstructive Sleep Apnea Treatment View project CFD MODELING OF A ROTATING ARC PLASMA REACTOR," 2014, doi: 10.13140/RG.2.2.20874.13768.
22. N. Yu, Y. Yang, R. Jourdain, M. Gourma, A. Bennett, and F. Fang, "Design and optimization of plasma jet nozzles based on computational fluid dynamics", doi: 10.1007/s00170-020-05568-4/Published.
23. M. Mortazavi, L. Amato, N. Manivannan, M. Abbod, and W. Balachandran, "Modelling of Electric Field Distribution in A Non-thermal Plasma Reactor Using COMSOL Multiphysics."
24. S. Sobhansarbandi, L. Maharjan, B. Fahimi, and F. Hassanipour, "Thermal fluid analysis of cold plasma methane reformer," *Fluids*, vol. 3, no. 2, Jun. 2018, doi: 10.3390/fluids3020031.
25. D. Lašič Jurković, J. L. Liu, A. Pohar, and B. Likozar, "Methane Dry Reforming over Ni/Al2O3 Catalyst in Spark Plasma Reactor: Linking Computational Fluid Dynamics (CFD) with Reaction Kinetic Modelling," *Catal Today*, vol. 362, pp. 11–21, Feb. 2021, doi: 10.1016/j.cattod.2020.05.028.
26. C. Mas-Peiro, H. Quinteros-Lama, J. O. Pou, and F. Llovell, "Thermodynamic Characterization of Gas Mixtures for Non-Thermal Plasma CO2 Conversion Applications with Soft-SAFT," *J Chem Eng Data*, vol. 68, no. 6, pp. 1376–1387, Jun. 2023, doi: 10.1021/acs.jced.3c00131.
27. I. I. I. Alkhatib, L. M. C. Pereira, J. Torne, and L. F. Vega, "Polar soft-SAFT: theory and comparison with molecular simulations and experimental data of pure polar fluids," *Phys Chem Chem Phys*, vol. 22, no. 23, pp. 13171–13191, 2020, doi: 10.1039/d0cp00846j.
28. C. Mas-Peiro, F. Llovell, and J. O. Pou, "Computational Fluid Dynamic (CFD) study of gas mixtures in a Non-Thermal Plasma for CO2 conversion," in *15th Mediterranean Congress of Chemical Engineering*

(MeCCE-15) Abstracts Publication, Grupo Pacífico, Jan. 2023. doi: 10.48158/MeCCE-15.T4-O-27.
29. A. Sobachkin, "Numerical Basis of CAD-Embedded CFD," 2014.
30. C. Mas-Peiro, J. O. Pou, and F. Llovell, "Thermodynamic characterization of gas mixtures for CCUS applications," in *14th Mediterranean Congress of Chemical Engineering (MeCCE14) Abstracts Publication*, Grupo Pacífico, Aug. 2020. doi: 10.48158/MeCCE-14.DG.07.05.
31. "Libro del Web de Química del NIST." https://webbook.nist.gov/chemistry/ (accessed May 08, 2020).